

## Universal Dynamical Scaling of Quasi-Two-Dimensional Vortices in a Strongly Interacting Fermionic Superfluid

Xiang-Pei Liu,<sup>1,2,3,\*</sup> Xing-Can Yao<sup>1,2,3,\*</sup>, Youjin Deng,<sup>1,2,3,4,\*</sup> Xiao-Qiong Wang,<sup>1,2,3</sup> Yu-Xuan Wang,<sup>1,2,3</sup>  
Chun-Jiong Huang<sup>1,2</sup>, Xiaopeng Li,<sup>5,6</sup> Yu-Ao Chen<sup>1,2,3</sup> and Jian-Wei Pan<sup>1,2,3</sup>

<sup>1</sup>*Hefei National Laboratory for Physical Sciences at the Microscale and Department of Modern Physics, University of Science and Technology of China, Hefei 230026, China*

<sup>2</sup>*Shanghai Branch, CAS Center for Excellence in Quantum Information and Quantum Physics, University of Science and Technology of China, Shanghai 201315, China*

<sup>3</sup>*Shanghai Research Center for Quantum Sciences, Shanghai 201315, China*

<sup>4</sup>*MinJiang Collaborative Center for Theoretical Physics, College of Physics and Electronic Information Engineering, Minjiang University, Fuzhou 350108, China*

<sup>5</sup>*State Key Laboratory of Surface Physics, Institute of Nanoelectronics and Quantum Computing, and Department of Physics, Fudan University, Shanghai 200433, China*

<sup>6</sup>*Collaborative Innovation Center of Advanced Microstructures, Nanjing 210093, China*

 (Received 29 January 2020; revised 2 September 2020; accepted 7 April 2021; published 6 May 2021)

Vortices play a leading role in many fascinating quantum phenomena. Here we generate a large number of vortices by thermally quenching a fermionic superfluid of  ${}^6\text{Li}$  atoms in an oblate optical trap and study their annihilation dynamics and spatial distribution. Over a wide interaction range from the attractive to the repulsive side across the Feshbach resonance, these quasi-two-dimensional vortices are observed to follow algebraic scaling laws both in time and space, having exponents consistent with the two-dimensional universality. We further simulate the classical  $XY$  model on the square lattice by a Glauber dynamics and find good agreement between the numerical and experimental behaviors. Our work provides a direct demonstration of the universal 2D vortex dynamics.

DOI: [10.1103/PhysRevLett.126.185302](https://doi.org/10.1103/PhysRevLett.126.185302)

Quantized vortices, topological defects in a superfluid, lie at the cornerstone of describing collective phenomena and phase transitions [1,2]. In three dimensions (3D), as the temperature  $T$  is raised, the excited vortex lines or loops proliferate and transform the superfluid into the normal state through a second-order thermodynamic phase transition. In 2D, the vortices and antivortices in a superfluid form tight pairs, and as  $T$  rises, they break up at the celebrated Berezinskii-Kosterlitz-Thouless (BKT) phase transition [3–5].

With a high degree of manipulations and tunabilities, ultracold atomic gases provide an ideal platform for studying vortices. Vortex lattices have been generated and their equilibrium properties have been intensively studied [6–13]. The spontaneous formation of vortices in a Bose condensation has been generated via the Kibble-Zurek mechanism [14,15]. These vortices can display rich dynamics, including nonexponential decay [16], transport and reconnection of vortex filaments [15,17], Kolmogorov energy cascade [18,19], giant vortex clustering [20,21], and so on.

Spontaneous vortices have also been successfully generated in fermionic superfluid by thermally quenching across the superfluid transition [22,23], and the dependence of the number of generated vortices on the quench rate is shown to be governed by the universal Kibble-Zurek

mechanism. An important question is then how these vortices annihilate afterward. A quantum vortex can disappear by drifting out of the superfluid or colliding with another vortex with opposite polarity. The former is a one-body process, giving the traditional exponential decay of vortex number [9,10]. It was argued [24,25] that, depending on the presence or absence of dissipation, the vortex-pair annihilation can be a two- or four-body process. The corresponding decaying dynamics is a power law with exponent  $-1$  or  $-1/3$ , respectively.

From universality, the dynamics of vortices can be studied within the Ginzburg-Landau (GL) theory, a phenomenological theory of superfluidity. In 2D, the dynamics of vortices following a rapid thermal quench were numerically investigated [26] by simulating the classical  $XY$  spin model, a simplified lattice model for the GL theory. The number of vortices was observed to decay algebraically as  $\propto [t/\log(t)]^{-1}$ , where  $t$  is the time after the quench. The logarithmic correction  $\log t$ , arising from the effective Coulomb interaction ( $\propto 1/r$ ) between two vortices of distance  $r$ , was successfully identified. In addition, the average distance  $\xi(t)$  between neighboring vortices was found to increase approximately as  $t^{1/2}$  and the vortex-antivortex spatial correlation function obeys another power law  $C(r) \propto r^{-3}$  for  $r \gg \xi(t)$ .

In this Letter, we study the vortex-annihilation dynamics following a rapid thermal quench of a strongly interacting Fermi gas of  ${}^6\text{Li}$  atoms in an oblate optical trap through the superfluid phase transition. Because of the oblate trap geometry, the vortices have strong tendency to be aligned along the tightly confined direction and are thus quasi-two-dimensional (quasi-2D), as confirmed by high-contrast imaging of vortex cores. The configuration after the thermal quench consists of an equal number of randomly distributed vortices and antivortices. At unitarity, as well as at the Bose-Einstein condensates (BEC) and the Bardeen-Cooper-Schrieffer (BCS) side, we observe that the number density of quasi-2D vortices algebraically decays approximately as  $t^{-1}$  with  $t$  the holding time. Apart from the logarithmic correction, this is consistent with the annihilation dynamics of vortices in the 2D  $XY$  model [26]. Further, we find that the probability distribution of the distance  $r$  between neighboring vortices obeys another power law  $r^{-3}$  and the average distance increases as  $t^{1/2}$ . Following Ref. [26], we simulate the  $XY$  model on the square lattice, and observe that the real-time dynamics in experiment and the dynamics in simulation exhibit very similar behaviors. This suggests that the coarse-grained GL theory can provide a precise description of the dynamics of quasi-2D vortices in our oblate system.

The main experimental setup and method to prepare  ${}^6\text{Li}$  superfluid have been described in our previous work [13,22]. A balanced spin mixture of  ${}^6\text{Li}$  with  $1 \times 10^7$  atoms is first loaded into an elliptical optical trap [wavelength 1064 nm,  $1/e^2$  radius 200 and  $48 \mu\text{m}$  (gravity direction)] at 832.18 G. Then, the magnetic field is adiabatically ramped to the final value (or held at 832.18 G), and the cloud is evaporatively cooled by ramping-down the laser power. At unitarity, the final trap frequencies are  $(\omega_x, \omega_y, \omega_z) = 2\pi \times (56.2, 218.4, 16.7)$  Hz, where  $\omega_z$  is provided by the residual magnetic curvature. Using a moderate ramp time of 400 ms, the cloud temperature can be effectively quenched through the superfluid phase transition, and thus plenty of vortices and antivortices are spontaneously generated.

After trap ramping, the system is held until the quasi-condensate number is saturated. At this point, the spontaneous vortices are found to be clearly visible [22], and the initial time ( $t = 0$ ) is defined for the study of vortex dynamics. Afterward, the optical trap is switched off and the magnetic field is jumped to 720 G for a series of time  $t$ , and the cloud is probed after 10 ms expansion with absorption imaging. By fitting the measured density profile to a Gaussian plus Thomas-Fermi distribution, we obtain an approximate estimate of the cloud temperature to be  $T \approx 0.09T_F$  [27]. Typical results for the spontaneous vortices probed at  $t = 0$  are shown in the first column of Fig. 1. It is found that all these high-contrast vortex cores are randomly distributed in the BCS-BEC crossover.

*Annihilation dynamics.*—The randomly distributed vortices and antivortices imply that the system is in an

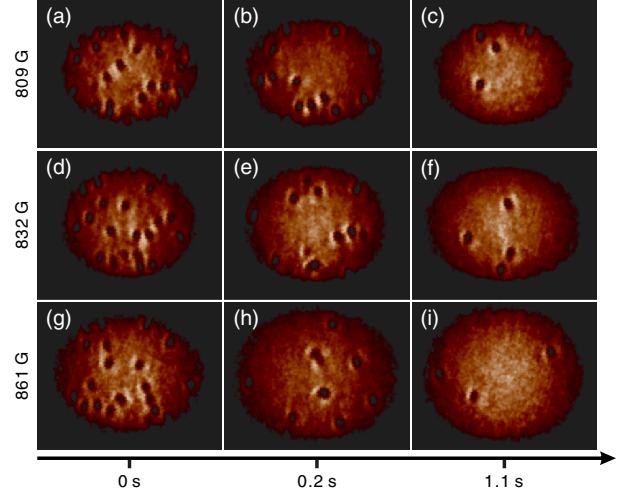


FIG. 1. Exemplary pictures of spontaneous vortices after different holding times in the BEC-BCS crossover. The experiments are performed at 809 G (a)–(c), 832 G (d)–(f), and 861 G (g)–(i), respectively, with a 400 ms ramp time. The initial time  $t = 0$  is defined as the quasi-condensate number reaches saturation. Each picture has a size of  $440 \times 350 \mu\text{m}^2$ .

out-of-equilibrium state. It will approach equilibrium and establish the global superfluid phase coherence through a coarsening process, which is mainly due to the pairing and annihilation of vortex and antivortex. We carry out a series of measurements on the evolution of vortex density  $\rho_v$  at the BEC (809 G), unitarity (832 G), and BCS (861 G) regimes. Figure 1 shows typical images of vortices probed at 0, 0.2, and 1.1 s, respectively. A striking feature is that most of the vortices disappear after 1 s, implying the short lifetime of these spontaneous vortices. Figure 2 gives the statistical results of the time-dependent vortex densities. It is seen that the experimental data, while clearly deviating from an exponential form, can be well described by an algebraic scaling as

$$\rho_v = [a/(t + \Delta t)]^\zeta, \quad (1)$$

where an offset  $\Delta t$  is to account for short-time behavior. The fits give the dynamic exponent  $\zeta = 0.93 \pm 0.06$ ,  $0.93 \pm 0.15$ , and  $0.94 \pm 0.17$ , respectively for 809, 832, and 861 G, which agree well with each other within error bars. The decay of the vortex number, at the unitarity, the BEC, and the BCS side, all displays power-law decaying behaviors and further shares the same exponent, strongly indicating some universal underlying mechanism. In addition, we find that this power-law scaling behavior is independent of the thermal ramping rate and the final trap frequencies. In other words, the universal vortex dynamics does not depend on the final superfluid temperature, as long as it is below the superfluid phase transition.

Our oblate fermionic system is essentially 3D, since the Fermi energy is much higher than  $\hbar\omega_y$ . Thus, unlike in the

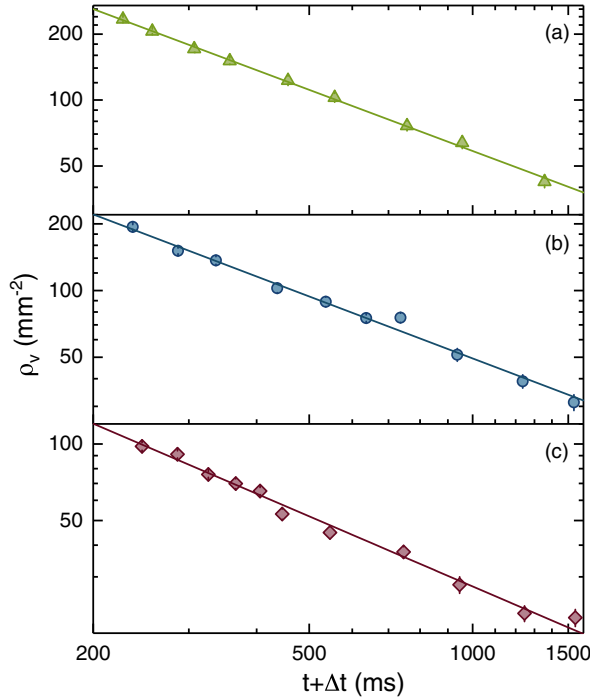


FIG. 2. Annihilation dynamics of quasi-2D vortices for (a), 809 G, (b), 832 G, and (c), 861 G. The ramp time is 400 ms. The vertical axis is the number density of vortices  $\rho_v$ , where each point, with a standard statistical error, is acquired by averaging 30 repetitive measurements. The solid lines are the fitting curves with power-law function, and  $\Delta t$  represents the time offset, with  $\Delta t = 227 \pm 28$  ms for (a),  $237 \pm 70$  ms for (b), and  $246 \pm 80$  ms for (c).

real 2D plane where the condensate is absent, the superfluid in our system mainly comes from the condensation of molecules or Cooper pairs. However, due to the oblate trap geometry, the minimum energy cost to generate a vortex loop is on the order of  $2\pi \times 218$  Hz, and is at least 4 times higher than that for a vortex line along the gravity ( $y$ ) direction, giving a much larger probability for the latter. In our finite system with tens of vortices, most of the vortices are thus expected to be vertically aligned. This is confirmed by the high-contrast imaging of vortex cores along the gravity direction, and also qualitatively by the numerical simulation of the Gross-Pitaevskii equation [28]. These vertically aligned vortices likely maintain their quasi-2D structures during the annihilation process, and, in a coarse-grained treatment, other mesoscopic details play as irrelevant perturbative roles. We thus argue from universality that the dynamics of these quasi-2D vortices can be described by the 2D GL theory. Assuming a two-body process for the vortex annihilation, one can simply write down a mean-field description as  $d\rho_v/dt = -\kappa\rho_v^2$ , with  $\kappa$  a constant, giving a power-law decay  $\rho_v(t) \propto 1/t$  [29]. A more advanced treatment would require us to consider the spatial structure of vortices and the effective Coulomb interaction, which is inversely proportional to the distance  $r$  between vortices as  $\propto 1/r$ . From the numerical integration

of the field-theoretical equation, it was obtained that a logarithmic correction would arise and the dynamics is modified as  $\rho_v(t) \propto (t/\log t)^{-1}$  [26,29,30].

We follow Ref. [26] and consider a single-site Glauber dynamics [38,39] by simulating the classical square-lattice XY model [28], of which the BKT phase transition is known to occur at temperature  $k_B T_{\text{BKT}} = 0.89$  ( $k_B$  is the Boltzmann constant) [26]. A random spin configuration is prepared and instantly quenched to  $k_B T = 0.2$ , where the system is in a deep superfluid phase. The Glauber dynamics follows by choosing a random spin and rotating it by a randomly chosen phase according to the Metropolis rule. Figure 3(a) shows snapshots of vortex configurations for a system size of  $L = 200$  at various times after the thermal quench. Here the “time” unit corresponds to one averaged updating step per spin. We then measure the temporal evolution of vortex density  $\rho_v$  over 400 independent runs, and the results are shown in Fig. 3(b). Finite size effects are clearly observed, as the vortex densities gradually deviate the power-law scaling for  $t \gg 1$ . For a large system size of  $L = 600$ , the results are well consistent with the theoretical prediction  $(t/\log t)^{-1}$  [28] for  $t \gg 1$ . For mediate time  $t \in O(10)$ ,  $\rho_v$  decays approximately as  $1/t$ , which looks surprisingly similar to the real-time dynamics of the experiment, as shown in the inset of Fig. 3(b).

The equilibrium behavior at  $T < T_{\text{BKT}}$  is related to low-energy phonon or spin-wave excitations and has a

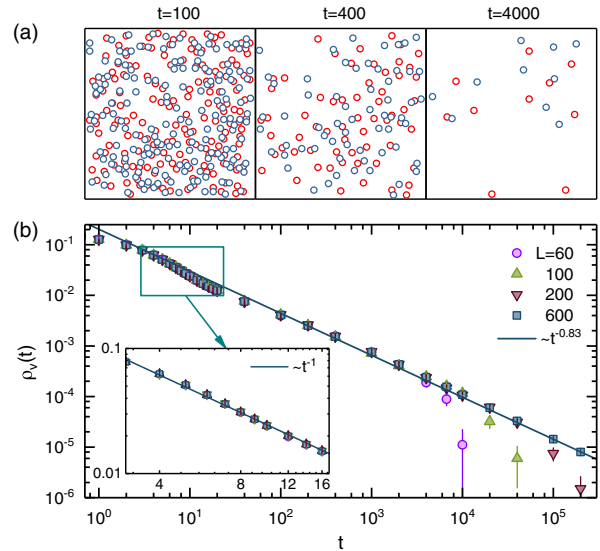


FIG. 3. Glauber dynamics of the 2D XY model from Monte Carlo simulations. (a) Snapshots of vortex configuration at various time  $t$  after the quench, with red and blue circles being vortices and antivortices, respectively. The system size is  $L = 200$ . (b) Time dependence of the vortex density  $\rho_v$  after the quench, with different symbols representing system sizes. The short-time behavior of decay dynamics (shown in the inset) displays a power-law decay with an exponent about  $-1$ . The longtime algebraic decay with exponent  $-0.83$  is consistent with  $(t/\log t)^{-1}$  [28].

$T$ -dependent critical exponent for the order parameter. In contrast, the universal vortex dynamics, decoupled from the low-energy excitations, is  $T$  independent. This robustness is well demonstrated by our experimental results for different ramping rates as well as numerical simulations at various temperatures.

*Spatial distribution.*—In 2D, the effective Coulomb interaction introduces a logarithmically diverging energy  $\propto \log r$  for a pair of vortices of distance  $r$ , and thus the vortices are tightly bound below the BKT transition. In the vortex-annihilation dynamics, the effective interaction gives rise to a logarithmic correction that is beyond the mean-field description, which, unfortunately, our experiment fails to identify. However, as shown in Ref. [26], the vortices can display rich spatial information from the GL theory. We measure pair correlation functions that ignore the vortex polarity, since our images cannot tell the polarity of vortices. We sequentially visit each vortex, pair it with its nearest-neighboring vortex, and record their distance  $r$  (in this procedure, a vortex might be paired more than once). For each set of parameters, 300 repetitive experiments are performed, and the histogram of such pairing distance  $r$  is measured. The results are shown in Fig. 4(a), where  $P(r)dr$  represents the probability for distance  $(r, r + dr)$ , irrespective of angular dependence. As expected, the pairing distance has a characteristic value  $r_0$ , with  $P(r)$  dropping rapidly for small  $r < r_0$ . The length scale  $r_0 \approx 30 \mu\text{m}$  is consistent with the typical size of vortex cores in Fig. 1, as measured from the density distribution. An intriguing property is that a flat-tail distribution occurs for large  $r$ , indicating a power-law decay  $P(r) \sim r^{-\eta}$  for  $r \gg r_0$ . Indeed, we find that the data for  $r \geq r_0$  are well described by a simple ansatz  $P(r) = a/r^\eta$ , and the exponent is estimated to be  $\eta = 3.00 \pm 0.30$ ,  $3.26 \pm 0.20$ , and  $3.29 \pm 0.18$  for 809, 832, and 861 G, respectively. A typical Monte Carlo result for the 2D XY model is shown in the inset of Fig. 4(a), displaying similar behavior as the experiment, for which the fit gives  $\eta = 2.92 \pm 0.15$ .

From the probability distribution  $P(r)$ , we calculate the average distance between neighboring vortices  $\xi(t)$  as a function of holding time  $t$ . The approximate scaling behavior  $\xi^2 \propto t$  in Fig. 4(b) provides another piece of evidence that the annihilation dynamics of quasi-2D vortices in our oblate system can be described by the coarse-grained GL theory for 2D superfluidity.

Universality is a fundamental concept in the modern theory of phase transition and critical phenomena, revealing common macroscopic properties for seemingly disparate systems. According to the renormalization group theory, the universality solely depends on a small number of global features of the system, including the spatial dimensionality, the symmetry of the interaction and the order parameter, etc. In our fermionic superfluid cloud, the constituent particles are either bosonic molecules or fermionic

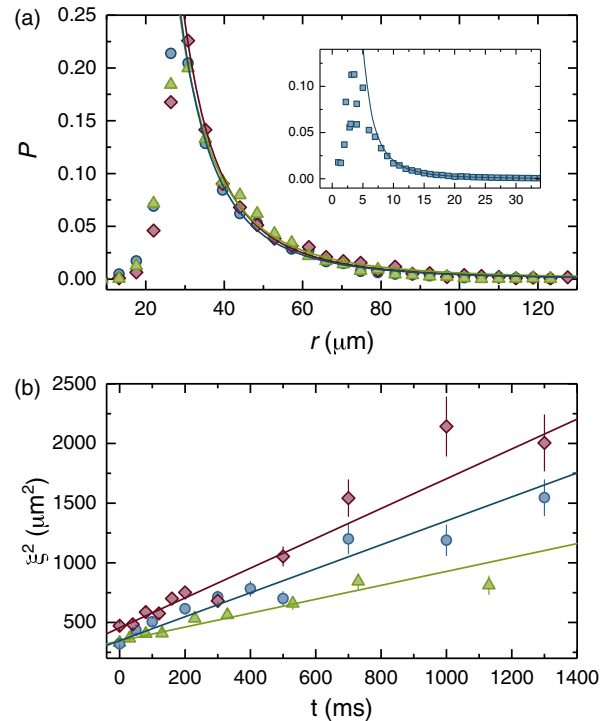


FIG. 4. (a) Probability distribution of the vortex distance for 809 G (green triangle), 832 G (blue circle), and 861 G (red diamond). Each set of data comes from 300 repetitive measurements. The solid lines are the power-law fitting curves. The inset displays a simulation result for the XY model. (b) Temporal evolution of average squared distance between neighboring vortices for 809 G (green triangle), 832 G (blue circle), and 861 G (red diamond). Each set of data comes from 30 repetitive measurements. The solid lines are the linear fitting curves.

Cooper pairs, and the interatomic interactions can be repulsive, attractive, or resonant. These microscopic features are very different from the classical spins in the XY model, which are of unit length, live on lattice sites, and interact through nearest-neighbor coupling. The mesoscopic structures in the experimental system are also much more complex. The ratios of our trap frequencies along the tightly confined and the other two directions are about 4 and 13. As a consequence, the thermal quench may produce small closed vortex loops in addition to the vertically vortex lines; the equilibrium superfluid, established through the coarsening process of vortex annihilation, corresponds to a BEC that has long-ranged order, instead of quasi-long-ranged order in real 2D. Therefore, the observed common universal dynamical properties of quasi-2D and 2D vortices in these two systems are surprising, and give a strong and direct demonstration of the dynamics universality class of 2D vortices.

In conclusion, by studying the dynamics of the quasi-2D vortices in a strongly interacting fermionic superfluid, we observe universal power-law scaling behaviors over a wide interaction range, i.e., at unitarity, the BEC, and the

BCS side, and find agreement between the experimental critical exponents and the theoretical predictions for generic 2D vortices. A close resemblance is further revealed between the experimental measurements and the numerical simulation of the classical  $XY$  model in 2D. According to the GL theory, the coefficient  $a$  in the algebraic decaying, Eq. (1), depends on temperature  $T$  and is proportional to the product  $\rho_s(T)\Gamma(T)$ , where  $\rho_s$  is the superfluidity stiffness and  $\Gamma$  is the kinetic coefficient. Therefore, it is possible to extract information for  $\rho_s$  from the vortex-annihilation dynamics by varying temperature and interaction range. By having a larger and more oblate system, one might achieve the challenging goal of identifying the logarithmic correction, which is an important feature in the dynamics of 2D vortices. We mention that besides the observed dynamical behaviors, the generated spontaneous vortices exhibit exotic quantum turbulence physics [40]. It is also fascinating and challenging to explore the crossover from the 3D thermodynamic phase transition to the 2D topological one by tuning the trap geometry to be more and more oblate. With a high stability and controllability, our experiment platform paves the way for studying these rich quantum phenomena of spontaneous vortices.

We thank J. Schmiedmayer for helpful discussions. This work is supported by the National Key R&D Program of China (Grants No. 2018YFA0306501, No. 2017YFA0304204, No. 2016YFA0301604), NSFC of China (Grants No. 11874340, No. 11425417, No. 117740067, No. 11625522), the Chinese Academy of Sciences (CAS), the Anhui Initiative in Quantum Information Technologies, the Shanghai Municipal Science and Technology Major Project (Grant No. 2019SHZDZX01), and the Fundamental Research Funds for the Central Universities (under Grant No. WK2340000081).

\*L. X.-P., Y. X.-C., D. Y. contributed equally to this work.

- [1] L. Onsager, *Nuovo Cimento* **6**, 279 (1949).
- [2] R. P. Feynman, in *Progress in Low Temperature Physics* (Elsevier, New York, 1955), Vol. 1, pp. 17–53.
- [3] V. Berezinskii, *Sov. Phys. JETP* **34**, 610 (1972).
- [4] J. M. Kosterlitz and D. J. Thouless, *J. Phys. C* **6**, 1181 (1973).
- [5] Z. Hadzibabic, P. Krüger, M. Cheneau, B. Battelier, and J. Dalibard, *Nature (London)* **441**, 1118 (2006).
- [6] K. W. Madison, F. Chevy, W. Wohlleben, and J. Dalibard, *Phys. Rev. Lett.* **84**, 806 (2000).
- [7] J. R. Abo-Shaer, C. Raman, J. M. Vogels, and W. Ketterle, *Science* **292**, 476 (2001).
- [8] I. Coddington, P. C. Haljan, P. Engels, V. Schweikhard, S. Tung, and E. A. Cornell, *Phys. Rev. A* **70**, 063607 (2004).

- [9] M. W. Zwierlein, J. R. Abo-Shaer, A. Schirotzek, C. H. Schunck, and W. Ketterle, *Nature (London)* **435**, 1047 (2005).
- [10] M. W. Zwierlein, A. Schirotzek, C. H. Schunck, and W. Ketterle, *Science* **311**, 492 (2006).
- [11] S. Giorgini, L. P. Pitaevskii, and S. Stringari, *Rev. Mod. Phys.* **80**, 1215 (2008).
- [12] A. L. Fetter, *Rev. Mod. Phys.* **81**, 647 (2009).
- [13] X.-C. Yao, H.-Z. Chen, Y.-P. Wu, X.-P. Liu, X.-Q. Wang, X. Jiang, Y. Deng, Y.-A. Chen, and J.-W. Pan, *Phys. Rev. Lett.* **117**, 145301 (2016).
- [14] C. N. Weiler, T. W. Neely, D. R. Scherer, A. S. Bradley, M. J. Davis, and B. P. Anderson, *Nature (London)* **455**, 948 (2008).
- [15] D. V. Freilich, D. M. Bianchi, A. M. Kaufman, T. K. Langin, D. S. Hall, and D. S. Hall, *Science* **329**, 1182 (2010).
- [16] W. J. Kwon, G. Moon, J. Choi, S. W. Seo, and Y. Shin, *Phys. Rev. A* **90**, 063627 (2014).
- [17] S. Serafini, L. Galantucci, E. Iseni, T. Bienaimé, R. N. Bisset, C. F. Barenghi, F. Dalfovo, G. Lamporesi, and G. Ferrari, *Phys. Rev. X* **7**, 021031 (2017).
- [18] T. Araki, M. Tsubota, and S. K. Nemirovskii, *Phys. Rev. Lett.* **89**, 145301 (2002).
- [19] T. W. Neely, A. S. Bradley, E. C. Samson, S. J. Rooney, E. M. Wright, K. J. H. Law, R. Carretero-González, P. G. Kevrekidis, M. J. Davis, and B. P. Anderson, *Phys. Rev. Lett.* **111**, 235301 (2013).
- [20] S. P. Johnstone, A. J. Groszek, P. T. Starkey, C. J. Billington, T. P. Simula, and K. Helmerson, *Science* **364**, 1267 (2019).
- [21] G. Gauthier, M. T. Reeves, X. Yu, A. S. Bradley, M. A. Baker, T. A. Bell, H. Rubinsztein-Dunlop, M. J. Davis, and T. W. Neely, *Science* **364**, 1264 (2019).
- [22] X.-P. Liu, X.-C. Yao, Y. Deng, X.-Q. Wang, Y.-X. Wang, X.-P. Li, Y.-A. Chen, and J.-W. Pan, arXiv:1902.07558v2.
- [23] B. Ko, J. W. Park, and Y. Shin, *Nat. Phys.* **15**, 1227 (2019).
- [24] G. W. Stagg, A. J. Allen, N. G. Parker, and C. F. Barenghi, *Phys. Rev. A* **91**, 013612 (2015).
- [25] A. W. Baggaley and C. F. Barenghi, *Phys. Rev. A* **97**, 033601 (2018).
- [26] A. Jelić and L. F. Cugliandolo, *J. Stat. Mech.* (2011) P02032.
- [27] R. Roy, A. Green, R. Bowler, and S. Gupta, *Phys. Rev. Lett.* **118**, 055301 (2017).
- [28] See Supplemental Material at <http://link.aps.org/supplemental/10.1103/PhysRevLett.126.185302> for details, which includes Refs. [4,29–37].
- [29] M. Mondello and N. Goldenfeld, *Phys. Rev. A* **42**, 5865 (1990).
- [30] A. J. Bray, A. J. Briant, and D. K. Jervis, *Phys. Rev. Lett.* **84**, 1503 (2000).
- [31] G. Huber and P. Alstrøm, *Physica (Amsterdam)* **195A**, 448 (1993).
- [32] B. Yurke, A. N. Pargellis, T. Kovacs, and D. A. Huse, *Phys. Rev. E* **47**, 1525 (1993).
- [33] A. D. Rutenberg and A. J. Bray, *Phys. Rev. E* **51**, 5499 (1995).
- [34] A. J. Bray, *Phys. Rev. E* **62**, 103 (2000).

- [35] J. M. Kosterlitz, *J. Phys. C* **7**, 1046 (1974).
- [36] A. Bulgac, M. M. Forbes, and P. Magierski, in *The BCS-BEC Crossover and the Unitary Fermi Gas* (Springer, Berlin, 2011), pp. 305–373.
- [37] A. Bulgac, Y.-L. Luo, P. Magierski, K. J. Roche, and Y. Yu, *Science* **332**, 1288 (2011).
- [38] R. J. Glauber, *J. Math. Phys. (N.Y.)* **4**, 294 (1963).
- [39] N. Metropolis, A. W. Rosenbluth, M. N. Rosenbluth, A. H. Teller, and E. Teller, *J. Chem. Phys.* **21**, 1087 (1953).
- [40] C. F. Barenghi, L. Skrbek, and K. R. Sreenivasan, *Proc. Natl. Acad. Sci. U.S.A.* **111**, 4647 (2014).